Ab Initio Study of the Reaction of CHO^+ with H_2O and NH_3

R. LÓPEZ, E. DEL RÍO, M. I. MENÉNDEZ, T. L. SORDO

Departamento de Química Física y Analítica, Facultad de Química, Universidad de Oviedo, C/Julián Clavería, 8, 33006 Oviedo, Principado de Asturias, Spain

Received 10 March 1999; accepted 7 May 1999

ABSTRACT: An MP4(full,SDTQ)/6-311++G(d,p)//MP2(full)/6-311++G(d,p) *ab initio* study was performed of the reactions of formyl and isoformyl cations with H_2O and NH_3, which play an important role in flame and interstellar chemistries. Two different confluent channels were located leading to $CO + H_3O^+/NH_4^+$. The first one corresponds to the approach of the neutral molecule to the carbon atom of the cations. The second one leads to the direct proton transfer from the cations to the neutrals. At 900 K the separate products $CO + H_3O^+/NH_4^+$ are the most stable species along the Gibbs energy profiles for the processes. For the reaction with H_2O the reaction channel leading to $HC(OH)_2^+$ (protonated formic acid) is disfavored with respect to the two $CO + H_3O^+$ channels in agreement with the experimental evidence that H_3O^+ is the major ion observed in hydrocarbon flames. According to our calculations, $NH_4^+ + H_2O$ are considerably more stable in Gibbs energy than $NH_3 + H_3O^+$; NH_4^+ will predominate in the reaction zone when ammonia is added to CH_4 + Ar diffusion flame, as experimentally observed. At 100 K the most stable structures are the intermediate complexes $CO\ldots HOH_2^+/HNH_3^+$. Particularly the $CO\ldots HOH_2^+$ complex has a lifetime large enough to be detected and, therefore, could play a certain role in interstellar chemistry. © 1999 John Wiley & Sons, Inc. J Comput Chem 20: 1432–1443, 1999

Keywords: *ab initio* calculations; hydrocarbon flames; interstellar chemistry; reaction channels; thermodynamic analysis

Correspondence to: T. L. Sordo; e-mail: tsg@dwarfl.quimica.uniovi.es

Contract/grant sponsor: DGUCYT (Spain); contract/grant number: PB94-1314-C03-01

CCC 0192-8651 / 99 / 131432-12

Introduction

The reactivity of formyl (HCO^+) and isoformyl (COH^+) cations is important in flames[1] and plasmas,[2] and plays a central role in the chemistry of interstellar clouds.[3]

The formyl cation is always observed in hydrocarbon flames, and generates many of the ions present in these systems. In this high density environment HCO^+ undergoes rapid proton transfer with H_2O to produce H_3O^+, the major ion observed in hydrocarbon flames. This positive ion–molecule reaction, which plays a role in hydrocarbon flame ionization, has an enthalpy of reaction as calculated from thermochemical data of -23 kcal/mol.[4a,b] A second reaction channel from $HCO^+ + H_2O$ to give $CH_3O_2^+$ has been also reported.[4] The experimental heat of reaction for this process has been reported to be -40 kcal/mol[4c] and -43 kcal/mol[4a], assuming that the $CH_3O_2^+$ species corresponds to protonated formic acid. On the other hand, it has been experimentally observed that when ammonia is added to a CH_4 + Ar diffusion flame[5] NH_4^+ predominates in the reaction zone. Under these circumstances the proton transfer between HCO^+ and NH_3 can play an important role as a source of NH_4^+.

It has been suggested that formation of formyl and isoformyl cations in interstellar space occurs mainly via the reaction of H_3^+ with CO. The most stable isomer, HCO^+, is predominantly produced.[6,7] Nevertheless, the generation of COH^+ in substantial proportions would have important consequences with regard to the modeling of the chemistry in interstellar clouds.[6] The reactions between formyl and isoformyl cations with water to produce $H_3O^+ + CO$ are important in this interstellar chemistry. Given that NH_3 has been detected in interstellar clouds (although it is unlikely to be present in large concentrations), the analogous reactions for the proton transfer between formyl and isoformyl cations and ammonia must also play a certain role in interstellar chemistry.

Previous high level *ab initio* calculations have predicted that HCO^+ and COH^+ are minimum energy linear structures, the former being the most stable one by about 37.7 kcal/mol.[8–10] The experimental value is about 38.2 kcal/mol.[11] The activation energy for the isomerization reaction $HCO^+ \rightarrow COH^+$ is theoretically predicted to be about 72.6 kcal/mol.[8,9] This energy barrier is substantially lower than the dissociation energy, and therefore, a significant number of ions may be able to undergo such rearrangement.[12] Very recently, the results of the catalytic action of small neutral molecules attached to the H atom in the rearrangement of HCO^+ into COH^+ have been reported.[9,13] In general, the interaction with a neutral molecule leads to a significant lowering of the barrier for the rearrangement. When the proton affinity of the neutral molecule lies above that of CO at carbon, as in the case of H_2O and NH_3, there is no successful catalysis of the rearrangement from HCO^+ to COH^+ because the proton is preferentially transferred to the neutral molecule rather than migrating to the O atom.

In the present work we performed an *ab initio* study of the mechanism of the following reactions:

$$HCO^+ + H_2O \rightarrow H_3O^+ + CO \quad (1)$$

$$COH^+ + H_2O \rightarrow H_3O^+ + CO \quad (2)$$

$$HCO^+ + NH_3 \rightarrow NH_4^+ + CO \quad (3)$$

and

$$COH^+ + NH_3 \rightarrow NH_4^+ + CO \quad (4)$$

in order to get a general understanding of their role in the chemistry of flames and interstellar clouds.

Methods

Ab initio calculations were performed with the GAUSSIAN 94 series of programs.[14] Stable species were fully optimized, and transition states (TSs) located using Schlegel's algorithm[15] at the MP2(full)/6-311 + + G(d,p) theory level.[16] All the critical points were further characterized, and the zero-point vibrational energies (ZPVEs) were evaluated by analytical computations of harmonic vibrational frequencies at the MP2(full)/6-311 + + G(d,p) level. Single-point calculations on the MP2(full)/6-311 + + G(d,p) geometries were also carried out at the MP4(full,SDTQ)/6-311 + + G(d,p) level.

MP2(full)/6-311 + + G(d,p) or MP2(full)/6-31G(d) Intrinsic Reaction Coordinate (IRC) calculations starting at each saddle point verified the two minima connected by that TS using the Gonzalez and Schlegel method[17] implemented in GAUSSIAN 94.

ΔH, ΔS and ΔG values were also calculated to obtain results more readily comparable with ex-

periment within the ideal gas, rigid rotor, and harmonic oscillator approximations.[18] A pressure of 1 atm and 100, 298.15, and 900 K of temperature were assumed in the calculations.

Atomic charges were determined using a Natural Bond Orbital (NBO) analysis.[19] *Ab initio* wave functions were analyzed by means of a theoretical method developed by Fukui's group[20] based on the expansion of the molecular orbitals (MOs) of a complex A-B in terms of those of its fragments. A configuration analysis is performed by writing the MO wave function of the combined system in terms of various electronic configurations

$$\psi = C_o \psi_o + \sum_q C_q \Psi_q \qquad (5)$$

where ψ_o (zero configuration, AB) is the state in which neither electron transfer nor electron excitation takes place, and ψ_q stands for monotransferred configurations (A^+B^- and A^-B^+), monoexcited configurations (A*B and AB*), and so on. The analysis of the wave function was performed using the ANACAL program.[21]

Results and Discussion

We present first the results obtained for the proton transfer from HCO^+ and COH^+ to H_2O and then the corresponding to the proton transfer to NH_3. Unless otherwise indicated, we will present in the text MP4(full,SDTQ)/6-311 + + G(d,p)//MP2(full)/6-311 + + G(d,p) energies including the MP2 ZPVE correction.

REACTIONS $CHO^+ + H_2O \rightarrow CO + H_3O^+$

Two different reaction channels appear for the attack of H_2O on both HCO^+ and COH^+. The first reaction channel corresponds to the interaction between the oxygen atom of water and the carbon atom of the cations. The second one corresponds to the direct transfer of a proton from the cations to H_2O. Figure 1 displays the optimized geometry of the critical structures located along the reaction coordinate for reactions 1 and 2. Table I collects the relative electronic energies of those structures.

Let us analyze first the results corresponding to the reaction of the formyl cation with H_2O (reaction 1). The first critical structure located along the first reaction channel is an intermolecular complex between HCO^+ and H_2O, **MA1**, which is 20.8 kcal/mol under the reactants. According to an NBO analysis, the net charge transfer from H_2O to the formyl cation, which has lost its linearity, is 0.05 e. This intermolecular complex can evolve through a TS, **TSA12**, with an energy barrier of 0.3 kcal/mol to give a minimum structure, **MA2**, which is 37.0 kcal/mol more stable than reactants (the corresponding G2** value is 36.8 kcal/mol[9]). Two main geometrical changes are observed when going from **MA1** to **TSA12**: the oxygen atom of the water molecule gets closer to the H atom in HCO^+, and this reactant recovers its linearity. The net charge transfer from H_2O at this TS is 0.03 e. At **MA2**, which has C_s symmetry, HCO^+ has transferred the proton to the water molecule. **MA2** can isomerize through a TS for inversion in the H_3O^+ moiety, **TSA22**, of C_{2v} symmetry with an energy barrier of 0.4 kcal/mol. Finally, **MA2** can also proceed directly to the products $CO + H_3O^+$, which are 22.6 kcal/mol under reactants (the corresponding G2** value is 22.5 kcal/mol[9]) in agreement with the greater proton affinity of H_2O than that of CO at C. The energy profile for the second channel corresponding to the direct proton transfer decreases monotonously without encountering any energy barrier to form **MA2**.

Concerning reaction 2, the first reaction channel leads to a minimum structure, **MA3**, of C_1 symmetry, which is 19.4 kcal/mol more stable than reactants. In **MA3**, the oxygen atom of the water molecule is bound to the carbon atom of the isoformyl cation forming an angle of 101.4° with the C—O bond. The H atom of the COH^+ moiety forms an angle of 109.3° with the same bond, and presents an outward orientation. The net charge transfer from the H_2O moiety to the COH^+ fragment is 0.38 e. **MA3** is connected with a minimum structure, **MA4**, 71.7 kcal/mol more stable than reactants (the corresponding G2** value is 68.9 kcal/mol[9]), through a TS, **TSA34**, with an energy barrier of 3.7 kcal/mol. At **TSA34** the H_2O molecule has moved to a distance of 2.465 Å away from the COH^+ fragment, which has recovered its linearity. At this TS the net charge transfer from H_2O is only 0.02 e, given that the distance between both fragments is relative large to facilitate the rotation of the isoformyl moiety. At **MA4** the isoformyl cation has transferred a proton to the water molecule determining a C_s symmetry. **MA4** can isomerize through a TS for inversion in the H_3O^+ moiety, **TSA44**, of C_{2v} symmetry with an energy barrier of 0.9 kcal/mol. **MA4** can also evolve directly to the products, $CO + H_3O^+$, which are 64.6 kcal/mol more stable than reactants. The second reaction channel for the direct

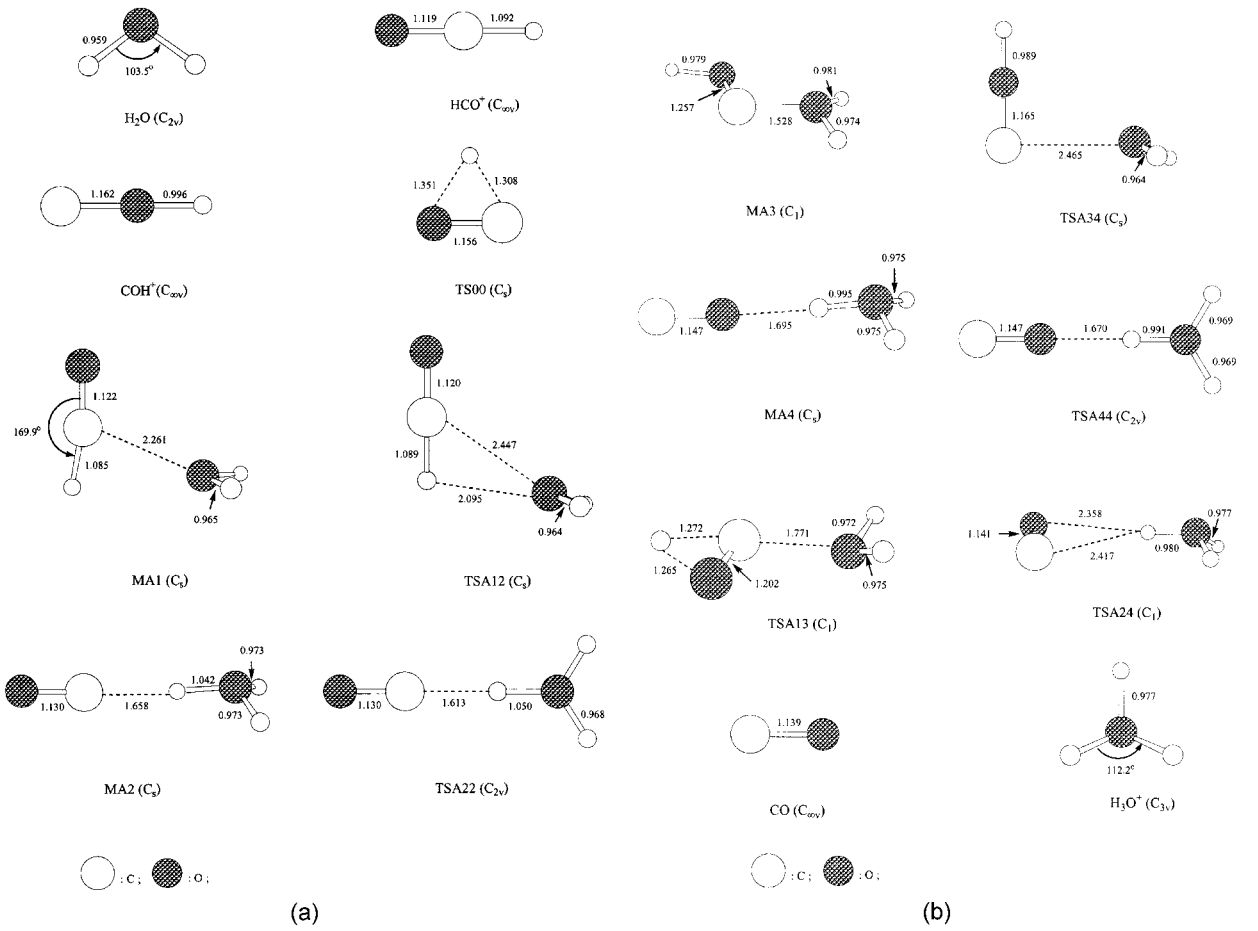

FIGURE 1. MP2(full) / 6-311 + + G(d,p) optimized geometries of the chemically important structures located for the reactions of formyl and isoformyl cations with H_2O. Bond lengths are given in angstroms and bond angles in degrees.

proton transfer gives **MA4** along a monotonously decreasing energy profile without encountering any energy barrier.

For both processes 1 and 2 the approach of the oxygen atom of water to the carbon atom of the cations leads to the formation of minimum energy structures through the interaction between the Next HOMO (NHOMO) of water and the LUMO of the cation (see Table II). However this interaction presents a smaller relative weight for **MA1**, where the HCO^+–H_2O system is mainly stabilized by electrostatic interaction between the oxygen atom of water and the carbon atom, which is the most positively charged atom in the formyl cation, both fragments being quite separate from each other. In effect, the total bond order between the fragments is only 0.051 at **MA1**. The search for a minimum energy structure presenting a stronger bonding between the O atom of water and the C atom of the formyl cation failed. No intermediate with the H atom oriented inwards was located for the COH^+–H_2O system.

Three TSs (**TS00**, **TSA13**, and **TSA24**) have been found directly connecting the energy profiles for reactions 1 and 2. **TS00** connects separate reactants of reactions 1 and 2 and corresponds to the isomerization of HCO^+ to COH^+. According to our calculations, **TS00** is 76.1 kcal/mol less stable than HCO^+, which in turn is 42.0 kcal/mol more stable than COH^+. These results are comparable with those obtained previously at MP2(full)/6-311 + + G(3df,3pd) (83.3 and 44.2 kcal/mol) and QCISD(T)(full)/6-311 + + G(2df,p)//B3LYP/6-311 + G(d,p) (73.9 and 38.8 kcal/mol) levels.[13] **TSA13** is 55.1 kcal/mol above $HCO^+ + H_2O$, and connects **MA1** with **MA3**. This is a saddle point for

TABLE I.

Relative MP2(full) / 6-311++G(d,p) Energies (ΔE_{elec}), Zero-Point Vibrational Energy Corrections (ZPVE), relative MP4(full,SDTQ) / 6-311++G(d,p) / / MP2(full) / 6-311++G(d,p) Energies (ΔE_{elec}), Enthalpies (ΔH), Entropy Corrections ($-T\Delta S$), and Gibbs' Free Energies (ΔG), in kcal / mol, of Chemically Important Structures for the Reaction of Formyl and Isoformyl Cations with H_2O.[a]

				T = 100 K			T = 298.15 K			T = 900 K		
Structure	ΔE_{elec}[b]	ZPVE	ΔE_{elec}[c]	ΔH	$-T\Delta S$	ΔG	ΔH	$-T\Delta S$	ΔG	ΔH	$-T\Delta S$	ΔG
$H_2O + HCO^+$	0.0	23.82	0.0	0.0	0.0	0.0	0.0	0.0	0.0	0.0	0.0	0.0
MA1	−22.5	25.61	−22.6	−21.3	2.2	−19.1	−21.3	6.8	−14.5	−19.9	18.1	−1.8
TSA12	−22.2	25.41	−22.1	−21.1	2.4	−18.7	−21.6	8.1	−13.5	−21.2	23.9	2.7
MA2	−38.6	26.40	−39.6	−37.6	2.5	−35.1	−37.9	8.0	−29.9	−37.2	23.2	−14.0
TSA22	−37.2	25.16	−37.9	−37.2	2.6	−34.6	−37.6	8.6	−29.0	−37.6	26.3	−11.3
H_3O^++ CO	−22.1	25.02	−23.8	−22.6	−0.2	−22.8	−22.6	−0.7	−23.3	−23.1	−1.2	−24.3
$H_2O + COH^+$	47.4	22.27	43.5	42.0	−0.02	42.0	42.4	−0.7	41.7	43.1	−3.4	39.7
MA3	21.5	27.32	19.1	21.9	2.6	24.5	21.2	9.2	30.4	21.9	27.0	48.9
TSA34	30.4	23.65	26.5	25.8	2.3	28.1	26.0	6.6	32.6	27.1	17.9	45.0
MA4	−29.8	26.48	−32.4	−30.2	2.3	−27.9	−30.2	7.0	−23.2	−29.3	19.6	−9.7
TSA44	−28.1	25.36	−30.4	−29.4	2.5	−26.9	−29.5	7.6	−21.9	−29.3	22.6	−6.7
H_2O + TS00	82.8	19.60	80.3	76.2	−0.4	75.8	76.3	−1.3	75.0	75.5	−2.7	72.8
TSA13	57.8	22.78	56.1	54.4	2.5	56.9	54.1	8.2	62.3	54.9	23.5	78.4
TSA24	−23.4	25.67	−25.2	−23.7	1.9	−21.8	−23.7	5.7	−18.0	−23.7	17.2	−6.5

[a] $\Delta H = \Delta E_{elec} + \Delta E_{ZPVE} + \Delta E_{thermal} + \Delta nRT$; thermal and ZPVE energies were obtained from the MP2(full) / 6-311++G(d,p) frequencies, while electronic contributions were derived from the MP4(full,SDTQ) / 6-311++G(d,p) single-point calculations.

[b] Relative MP2(full) / 6-311++G(d,p) energies.

[c] Relative MP4(full,SDTQ) / 6-311++G(d,p) / / MP2(full) / 6-311++G(d,p) energies.

the migration in the cationic fragment of the H atom from C to O. At **TSA13**, the H atom is halfway this motion interacting simultaneously with C and O atoms. Comparing **TSA13** with **TS00** we see that when a water molecule is attached to the C atom the TS for the migration of a H atom from C to O becomes tighter with shorter H—C and H—O distances (see Fig. 1). **TSA13** is 21.0 kcal/mol more stable than H_2O + **TS00**. Nevertheless, the presence of the water molecule does not seem to imply a greater electron transfer to the proton at the saddle point because the charge of the proton at **TS00** and **TSA13** is practically the same (+0.57, +0.59). When going from **MA1** to **MA3** through **TSA13** the C—OH_2 distance continuously decreases from 2.261 to 1.528 Å. The net charge transfer increases from 0.05 e at **MA1** to 0.25 e at **TSA13** and to 0.38 e at **MA3**. **TSA24** is 23.3 kcal/mol more stable than $HCO^+ + H_2O$ (the corresponding G2** value is 23.9 kcal/mol[9]) and 99.4 kcal/mol more stable than H_2O + **TS00**, and connects the ion-neutral complexes **MA2** and **MA4**. At **TSA24**, the proton detached from the C atom and solvated with the water molecule is placed approximately in front of the middle point of the C—O bond.

REACTIONS $CHO^+ + NH_3 \rightarrow CO + NH_4^+$

Two different reaction channels also appear for the attack of NH_3 on both HCO^+ and COH^+. The first reaction channel corresponds to the interaction between the nitrogen atom of ammonia and the carbon atom of the cations. The second one corresponds to the direct transfer of a proton to NH_3. Figure 2 displays the optimized geometry of the critical structures located along the reaction coordinate for reactions 3 and 4. Table III collects the relative electronic energies of those structures.

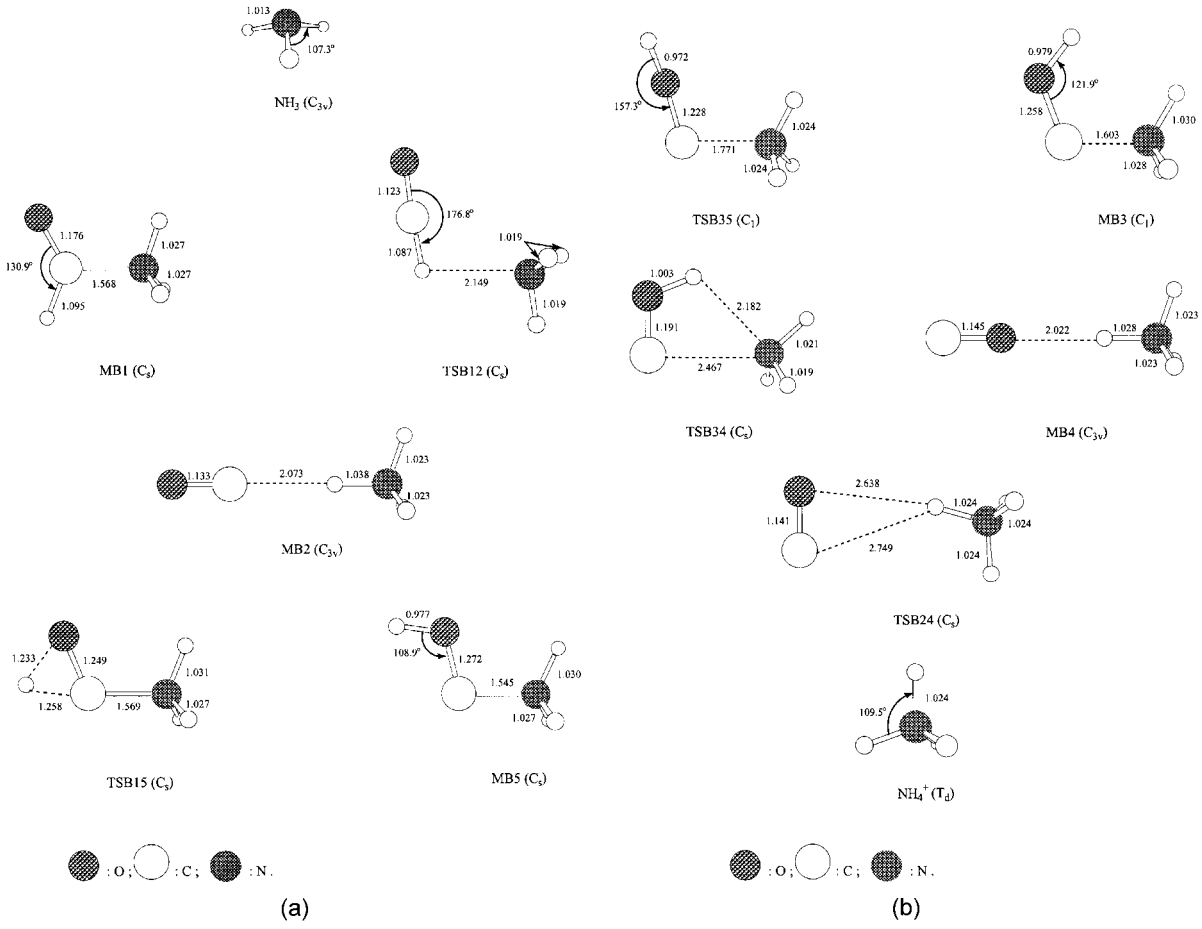

FIGURE 2. MP2(full) / 6-311++G(d,p) optimized geometries of the chemically important structures located for the reactions of formyl and isoformyl cations with NH_3. Bond lengths are given in angstroms and bond angles in degrees.

We shall first present the results corresponding to the proton transfer from the formyl cation to the ammonia molecule. When ammonia approaches the C atom of HCO^+, a minimum energy structure of C_s symmetry, **MB1**, appears 43.0 kcal/mol under reactants. In **MB1**, the nitrogen atom of ammonia is linked through its lone pair of electrons to the positively charged carbon atom of the formyl cation by a dative covalent bond with a bond distance of 1.568 Å. The HCO^+ fragment presents an H—C—O angle of 130.9°. The net charge transfer from ammonia is 0.58 e. **MB1** can evolve through a TS of C_s symmetry, **TSB12**, to give a minimum energy structure of C_{3v} symmetry, **MB2**. At **TSB12**, which is 19.4 kcal/mol above **MB1**, the nitrogen atom of ammonia is closer (2.149 Å) to the hydrogen atom of the formyl cation, which has almost completely recovered its linearity (the H—C—O angle is 176.8°). The net charge transfer from ammonia is only 0.05 e. At **MB2**, which is 69.1 kcal/mol more stable than reactants (the corresponding G2** value is 68.8 kcal/mol[9]), a proton has been transferred to the ammonia molecule originating an $OC\ldots H\text{-}NH_3^+$ complex with a C-proton distance of 2.073 Å. Finally, **MB2** can evolve directly to the products, $CO + NH_4^+$, which are 62.3 kcal/mol more stable than reactants (the corresponding G2** value is 62.1 kcal/mol[9]). The energy profile for the second channel corresponding to the direct proton transfer from the cation decreases monotonously without encountering any energy barrier to form **MB2**.

As for reaction 4, the approach of NH_3 to COH^+ along the first reaction channel can lead to two different minimum energy structures: **MB3** of C_1 symmetry and **MB5** of C_s symmetry. **MB3** is 32.4 kcal/mol more stable than reactants, while **MB5** is 12.3 kcal/mol more stable than **MB3**. In **MB3**, the nitrogen atom is bound to the carbon atom of the isoformyl cation with a bond length of 1.603 Å, and the isoformyl moiety presents a C—O—H angle of 121.9° with the hydrogen atom oriented inwards. This orientation determines a repulsion between that H and the H atom of the ammonia fragment that are separated by a distance of 2.236 Å. In **MB5**, the nitrogen atom is also bound to the carbon atom with a bond length of 1.545 Å and the C—O—H angle is 108.9°, with the hydrogen atom oriented outwards. This orientation avoids the H—H repulsion present in **MB3**, thus allowing a shorter C—N bond length and an important energy stabilization with respect to **MB3**. The net charge transfer from ammonia at **MB3** and **MB5** is 0.48 and 0.54 e, respectively (see Table II). **MB3** and **MB5** are connected each other through **TSB35** by rotation of the O—H bond about the C—O bond. **TSB35** is 10.9 kcal/mol less stable than **MB3**. At **TSB35**, the net charge transfer from ammonia is 0.38 e. **MB3** is connected with a minimum energy structure **MB4** through a TS, **TSB34**, with an energy barrier of 11.4 kcal/mol. At **TSB34**, the net charge transfer from ammonia is 0.06 e. The COH^+ moiety rotates about an axis perpendicular to the molecular plane and passing through the oxygen atom, to insert the hydrogen atom into the C—N bond and give **MB4**, which is a $CO\ldots H—NH_3^+$ complex 108.0 kcal/mol more stable than reactants (the corresponding G2** value is 104.2 kcal/mol[9]). **MB4** can evolve directly to the products $CO + NH_4^+$, which are 104.2 kcal/mol more

TABLE II.
Coefficients of the Most Important Electronic Configurations (A = HCO^+/COH^+, B = H_2O/NH_3), Most Important Changes in the Occupation Numbers of the Fragment MOs, $\Delta\nu$, Net Charge Transfer from H_2O/NH_3 to HCO^+/COH^+, CT, and Total Mayer Bond Orders Between the Fragments.

		MA1	MA3	MB1	MB3	MB5
	AB	0.9776	0.5967	0.4768	0.5162	0.4397
A^-B^+	**NHOMO-LUMO**	−0.1142	−0.2773			
	HOMO-LUMO	0.0260	0.0965	0.4232	−0.3859	−0.3949
$\Delta\nu$	**HOMO (B)**	−0.01	−0.11	−0.69	−0.62	−0.71
	NHOMO (B)	−0.04	−0.36	−0.02	−0.03	−0.03
	LUMO (A)	0.06	0.50	0.71	0.66	0.74
CT	**B → A**	0.05	0.38	0.58	0.48	0.54
Total Mayer bond order		0.051	0.588	0.639	0.578	0.622

TABLE III.

Relative MP2(full) / 6-311++G(d,p) Energies (ΔE_{elec}), Zero-Point Vibrational Energy Corrections (ZPVE), relative MP4(full,SDTQ) / 6-311++G(d,p) / / MP2(full) / 6-311++G(d,p) Energies (ΔE_{elec}), Enthalpies (ΔH), Entropy Corrections ($-T\Delta S$), and Gibbs' Free Energies (ΔG), in kcal / mol, of Chemically Important Structures for the Reaction of Formyl and Isoformyl Cations with NH_3.[a]

				T = 100 K			T = 298.15 K			T = 900 K		
Structure	ΔE_{elec}[b]	ZPVE	ΔE_{elec}[c]	ΔH	$-T\Delta S$	ΔG	ΔH	$-T\Delta S$	ΔG	ΔH	$-T\Delta S$	ΔG
$NH_3 + HCO^+$	0.0	32.08	0.0	0.0	0.0	0.0	0.0	0.0	0.0	0.0	0.0	0.0
MB1	−47.8	36.86	−47.8	−43.6	2.8	−40.8	−44.4	9.7	−34.7	−44.6	29.8	−14.8
TSB12	−24.8	33.32	−24.8	−24.1	2.4	−21.7	−24.4	7.7	−16.7	−24.0	22.7	−1.3
MB2	−71.5	35.87	−72.9	−69.6	2.5	−67.1	−69.6	7.5	−62.1	−69.0	21.9	−47.1
$NH_4^+ + CO$	−62.9	34.54	−64.7	−62.2	−0.1	−62.3	−62.3	−0.1	−62.4	−63.4	1.5	−61.9
$NH_3 + COH^+$	47.4	30.53	43.5	42.0	−0.02	42.0	42.4	−0.7	41.7	43.1	−3.4	39.7
MB3	8.4	35.92	5.7	8.9	2.8	11.7	8.2	9.7	17.9	8.6	28.8	37.4
TSB34	24.4	32.61	20.4	20.4	2.5	22.9	20.1	8.0	28.1	20.7	23.2	43.9
MB4	−67.0	35.46	−69.4	−66.4	2.5	−63.9	−66.1	7.1	−59.0	−65.4	19.3	−46.1
TSB35	22.3	33.10	19.4	19.9	2.7	22.6	19.6	8.5	28.1	20.1	24.9	45.0
MB5	−5.5	36.93	−7.6	−3.4	2.8	−0.6	−4.2	9.9	5.7	−4.2	30.2	26.0
NH_3 + TS00	82.8	27.86	80.3	76.2	−0.4	75.8	76.3	−1.3	75.0	75.5	−2.7	72.8
TSB15	32.2	32.78	31.0	31.1	2.8	33.9	30.4	9.6	40.0	30.3	29.5	59.8
TSB24	−63.4	34.98	−65.3	−62.7	1.7	−61.0	−62.6	5.1	−57.5	−63.1	16.0	−47.1

[a] $\Delta H = \Delta E_{elec} + \Delta E_{ZPVE} + \Delta E_{thermal} + \Delta nRT$; Thermal and ZPVE energies were obtained from the MP2(full) / 6-311++G(d,p) frequencies, while electronic contributions were derived from the MP4(full,SDTQ) / 6-311++G(d,p) single-point calculations.

[b] Relative MP2(full) / 6-311++G(d,p) energies.

[c] Relative MP4(full,SDTQ) / 6-311++G(d,p) / / MP2(full) / 6-311++G(d,p) energies.

stable than reactants. The second reaction channel for direct proton transfer from the cation gives **MB4**.

For the reaction of formyl and isoformyl cations with ammonia the interaction between the nitrogen atom and the carbon atom takes place through a charge transfer from the HOMO of ammonia to the LUMO of the cation (see Table II). Given that ammonia is a stronger base than water, the energy gap between the interacting fragment MOs is smaller now than in the case of reactions 1 and 2. As a consequence, the minimum energy structures formed and, in general, all the energy profile corresponding to the reaction between ammonia and formyl and isoformyl cations are considerably more stable than before. In **MB1**, **MB3**, and **MB5** the two fragments are separated by 1.55–1.60 Å, and the total bond order between them is 0.55–0.65 (see Table II). The energy barriers connecting **MB1** with **MB2**, and **MB3** with **MB4** are greater, respectively, than those connecting **MA1** with **MA2**, and **MA3** with **MA4**.

In addition to **TS00**, which connects separate reactants of reactions 3 and 4, two other TSs, **TSB15** and **TSB24**, have been found connecting the energy profiles for these reactions. **TSB15** connects **MB1** with **MB5**, and corresponds to the migration of the H atom in the cationic moiety from C to O. **TSB15** is 31.7 kcal/mol less stable than $HCO^+ + NH_3$, and 44.4 kcal/mol more stable than NH_3 + **TS00**. At this TS the net charge transfer from ammonia is 0.57 e. Comparing **TSB15** with **TS00**, we see that when an ammonia molecule is attached to the C atom the TS for the migration of an H atom from C to O becomes even tighter than **TSA13** with shorter H—C and H—O distances (see Fig. 2). Nevertheless, the presence of the ammonia does not cause a greater electron transfer to the proton at the saddle point because the charge of the proton at **TS00** and **TSB15** is very similar (+0.57, +0.60) despite the negative charge of the CO fragment. **TSB24** is 62.4 kcal/mol more stable than $HCO^+ + NH_3$ (the corresponding G2** value is 62.4 kcal/mol[9]) and 138.5 kcal/mol more stable than NH_3 + **TS00**, and connects the two complexes **MB2** and **MB4**. In **TSB24**, one of the hydrogen atoms of NH_4^+ is placed in front of the C—O bond with C—H and O—H distances of 2.749 and 2.638 Å, respectively (see Fig. 2).

According to an NBO analysis in both formyl and isoformyl cations C is the most positively charged atom (+0.92, and +1.0 e, respectively). Nevertheless, the H atom has a positive charge of +0.31 and +0.69 e, respectively. Therefore, although for all four processes direct proton transfer can take place without an energy barrier, the approach of the neutral molecule to the C atom of the cation could also play a certain role.

THERMODYNAMIC ANALYSIS

To discuss the role of reactions 1–4 in the chemistry of combustion and interstellar clouds we performed a thermodynamic analysis of our theoretical results at three different temperatures: 100, 298.15, and 900 K.

Figures 3 and 4 display the Gibbs energy profiles for reactions $CHO^+ + H_2O \rightarrow CO + H_3O^+$

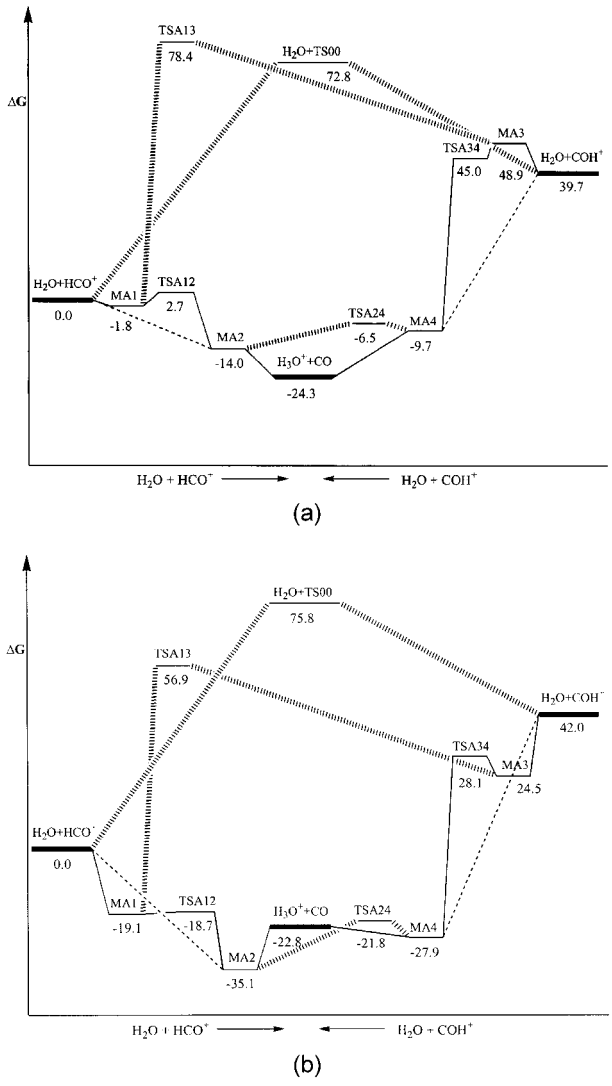

FIGURE 3. Gibbs energy profiles for the possible reaction channels (continuous and dashed lines) corresponding to the reaction of formyl and isoformyl cations with H_2O, and connections between them at (a) 900 K and (b) 100 K.

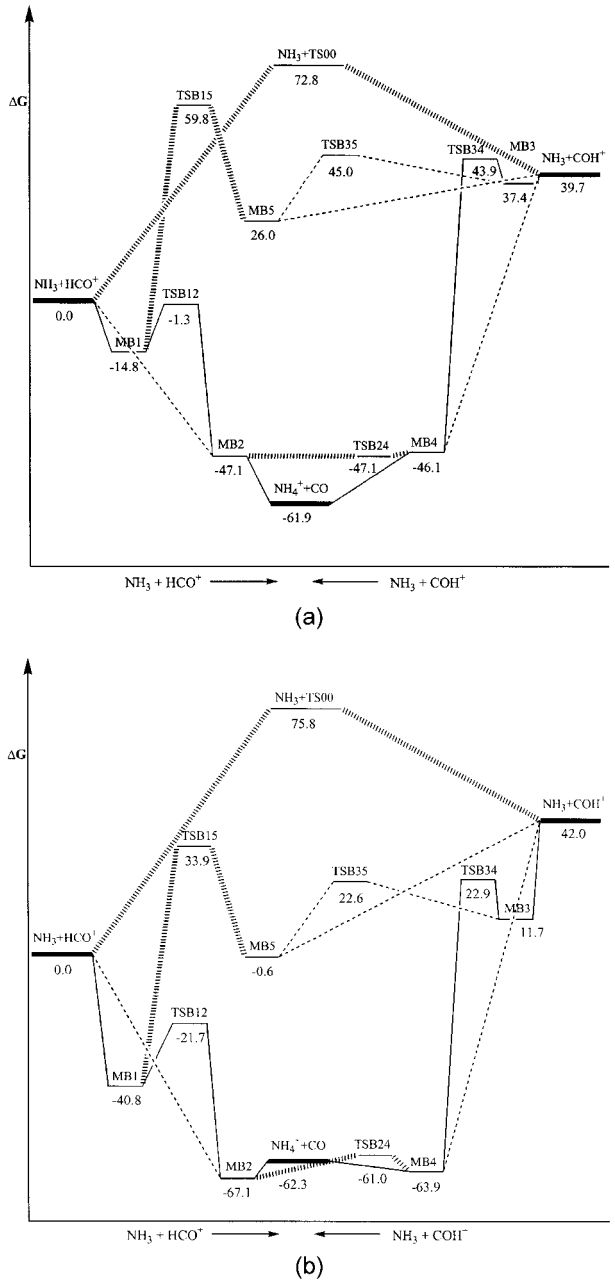

FIGURE 4. Gibbs energy profiles for the possible reaction channels (continuous and dashed lines) corresponding to the reaction of formyl and isoformyl cations with NH_3, and connections between them at (a) 900 K and (b) 100 K.

and $CHO^+ + NH_3 \rightarrow CO + NH_4^+$, respectively, at 900 and 100 K. Tables I and III collect ΔH, $-T\Delta S$ and ΔG for these processes at 100, 298.15, and 900 K.

The ΔH value predicted by our calculations for the reaction $HCO^+ + H_2O \rightarrow CO + H_3O^+$, -22.6 kcal/mol, is in good agreement with the experimental value of -23 kcal/mol.[4a,b] For the reaction $HCO^+ + H_2O \rightarrow HC(OH)_2^+$ (protonated formic acid) we obtained a ΔH of -33.8 kcal/mol to compare with the reported experimental values of -40 kcal/mol[4c] and -43 kcal/mol. The proton affinity difference between NH_3 and H_2O (the ΔH for the reaction $NH_4^+ + H_2O \rightarrow NH_3 + H_3O^+$) obtained by us is 39.7 kcal/mol (298.15 K) in good accordance with the reported experimental values: 34 ± 5 kcal/mol,[4b] 37.5 kcal/mol,[11b] and 38.5 kcal/mol.[22]

From Table I we see that, owing basically to the entropic contribution at 900 K, the Gibbs energy profiles for both reactions 1 and 2 are about 17–27 kcal/mol less stable with respect to $HCO^+ + H_2O$ than the electronic energy profiles except for **TS00** and products for which $-T\Delta S$ is -2.7 kcal/mol and -1.2 kcal/mol, respectively. This determines that products are the most stable species along the whole Gibbs energy profile (see Fig. 3a). Given that protonated formic acid is 21.5 kcal/mol less stable than $CO + H_3O^+$ in Gibbs energy, our calculations render at this temperature the reaction channel leading to protonated formic acid disfavored compared with that leading to $CO + H_3O^+$ in agreement with experimental evidence that H_3O^+ is the major ion observed in hydrocarbon flames. Analogously, Table III shows that at 900 K the entropic contribution makes the Gibbs energy profiles for reactions 3 and 4 less stable with respect to $HCO^+ + NH_3$ in general than the electronic energy profiles. **MB1**, **MB3**, **MB5**, and **TSB15** present a $-T\Delta S$ value of about 30 kcal/mol, whereas the remaining critical structures have a $-T\Delta S$ value of 16–25 kcal/mol approximately, except for **TS00** and products (1.5 kcal/mol). As a result, the products $CO + NH_4^+$ are the most stable species along the Gibbs energy profile for reactions 3 and 4 (see Fig. 4a). ΔG (900 K) for the reaction $NH_4^+ + H_2O \rightarrow NH_3 + H_3O^+$ is 37.6 kcal/mol, in agreement with the experimental observation that when ammonia is added to a CH_4 + Ar diffusion flame[5] NH_4^+ predominates in the reaction zone.

At 100 K as the $-T\Delta S$ term is about nine times smaller in absolute value than at 900 K, the separate products are not the most stable species along the Gibbs energy profiles for reactions 1–4. In effect, Figures 3b and 4b show that at 100 K for each of these reactions there is an intermediate corresponding to the interaction between a CO moiety and a protonated base fragment that is

more stable than products. Thus, **MB4** and **MB2** are 1.6 and 4.8 kcal/mol more stable than CO + NH_4^+, respectively, and **MA4** and **MA2** are 5.1 and 12.3 kcal/mol more stable than CO + H_3O^+, respectively, in Gibbs energy. Furthermore, our calculations predict that **MA2** could be detected in interstellar clouds and play a certain role in interstellar chemistry given that this intermediate has a lifetime of $3.67 \cdot 10^{14}$ s, much greater than that of the other three above-mentioned intermediates, which present a lifetime shorter than $7\ 10^{-2}$ s.[23]

In summary, the MP4(full,SDTQ)/6-311 + + G(d,p)//MP2(full)/6-311 + + G(d,p) study of the reaction between formyl and isoformyl cations with water and ammonia shows that these processes proceed through two different channels. The first one corresponds to the attack of the central atom of the neutral to the carbon atom of the cation, giving rise to a first intermediate. This evolves to give a second intermediate corresponding to the interaction of a CO molecule with the protonated neutral, which in turn, leads to the separate products. Along the second reaction channel the direct protonation of the neutral takes place to produce the second intermediate mentioned above. At 900 K, the separate products, CO + H_3O^+/NH_4^+, are the most stable species along the Gibbs energy profiles for the studied processes. Our theoretical results (−22.6 kcal/mol) reproduce quite well the ΔH for the reaction between formyl cation and water to give CO + H_3O^+ evaluated from experimental data (−23 kcal/mol). For the reaction channel giving protonated formic acid, our calculations predict a ΔH of reaction of −33.8 kcal/mol to compare with the experimental value of −40 kcal/mol. At 900 K, our calculations render the reaction channel, leading to protonated formic acid disfavored compared with that leading to CO + H_3O^+, in agreement with the experimental evidence that H_3O^+ is the major ion observed in hydrocarbon flames. According to our calculations, the ΔG (900 K) for the process $NH_4^+ + H_2O \rightarrow NH_3 + H_3O^+$ is 37.6 kcal/mol in agreement with the experimental observation that when ammonia is added to a CH_4 + Ar diffusion flame NH_4^+ predominates in the reaction zone. Unlike at 900 K, at 100 K the most stable structure located along the Gibbs energy profiles is the intermediate complex $CO \ldots HOH_2^+/HNH_3^+$ corresponding to the capture of a proton by the neutral. Particularly the $CO \ldots HOH_2^+$ complex is 12.3 kcal/mol more stable than CO + H_3O^+, and has a lifetime of $3.67 \cdot 10^{14}$ s and, consequently, according to our results, it could be a detectable species playing a certain role in interstellar chemistry.

Acknowledgments

The authors are grateful to DGICYT (Spain) for financial support (PB94-1314-C03-01). E. del R. also thanks to the DGICYT for a grant.

References

1. Warnatz, J. In Combustion Chemistry; Gardiner, W. C., Jr., Ed.; Springer, Berlin, 1984, p. 197.
2. Bohme, D. K.; Goodings, J. M.; Ng, C. W. Int J Mass Spectrom Ion Phys 1977, 24, 25.
3. Smith, D. Chem Rev 1992, 92, 1473.
4. (a) Calcote, H. F. In Ion-Molecule Reactions; Franklin, J. L., Ed.; Plenum: New York, 1972, p. 673, vol. 2; (b) Mackay, G. I.; Tanner, S. D.; Hopkinson, A. C.; Bohme, D. K. Can J Chem 1979; 57, 1518; (c) van Doren, J. M.; Barlow, S. E.; DePuy, C. H.; Bierbaum, V. M.; Dotan, I.; Ferguson, E. E. J Phys Chem 1986, 90, 2772.
5. (a) McAllister, T.; Nicholson, A. J. C. J Chem Soc Faraday Trans 1 1981, 77, 821; (b) McAllister, T. Aus J Chem 1984, 37, 511.
6. (a) Illies, A. J.; Jarrold, M. F.; Bowers, M. T. J Chem Phys 1982, 77, 5847; (b) Illies, A. J.; Jarrold, M. F.; Bowers, M. T. J Am Chem Soc 1983, 105, 2562.
7. Wagner−Redeker, W.; Kemper, P. R.; Jarrold, M. F.; Bowers, M. T. J Chem Phys 1985, 83, 1121.
8. (a) Martin, J. M. L.; Taylor, P. R.; Lee, T. J. J Chem Phys 1993, 99, 286, 9326; (b) Yamaguchi, Y.; Richards, C. A., Jr.; Schaefer, H. F., III. J Chem Phys 1994, 101, 8945.
9. Chalk, A. J.; Radom, L. J Am Chem Soc 1997, 119, 7573.
10. Mladnevic, M.; Schmatz, S. J Chem Phys 1998, 109, 4456.
11. (a) Freeman, C. G.; Knight, J. S.; Love, J. G.; McEwan, M. J. Int J Mass Spectrom Ion Process 1987, 80, 255; (b) Lias, S. G.; Bartmess, J. E.; Liebman, J. F.; Holmes, J. L.; Levin, R. D.; Mallard, W. G. J Phys Chem Ref Data Suppl 1988, 17; (c) Harland, P. W.; Kim, N. D.; Petrie, S. A. H. Aust J Chem 1989, 42, 9.
12. Burgers, P. C.; Holmes, J. L.; Mommers, A. A. J Am Chem Soc 1985, 107, 1099.
13. Cunje, A.; Rodriguez, C. F.; Bohme, D. K.; Hopkinson, A. C. J Phys Chem A 1998, 102, 478.
14. Frisch, M. J.; Trucks, G. W.; Schlegel, H. B.; Gill, P. M. W.; Johnson, B. G.; Robb, M. A.; Cheesman, J. R.; Keith, T. A.; Petersson, G. A.; Montgomery, J. A.; Raghavachari, K.; Al-Lahan, M. A.; Zakrzewski, V. G.; Ortiz, J. V.; Foresman, J. B.; Cioslowski, J.; Stefanov, B. B.; Nanayakkara, A.; Challacombe, M.; Peng, C. Y.; Ayala, P. Y.; Chen, W.; Wong, M. W.; Andres, J. L.; Replogle, E. S.; Gomperts, R.; Martin, R. L.; Fox, D. J.; Binkley, J. S.; Defrees, D. J.; Baker, J.; Stewart, J. P.; Head−Gordon, M.; Gonzalez, C.; Pople, J. A. Gaussian 94; Gaussian, Inc.: Pittsburgh, PA, 1995.
15. Schlegel, H. B. J Comput Chem 1982, 3, 211.
16. (a) Krishnan, R.; Binkley, J. S.; Seeger, R.; Pople, J. A. J Chem Phys 1980, 72, 650; McLean, A. D.; Chandler, G. S. J

Chem Phys 1980, 72, 5639; (c) Chandrasekhar, J.; Andrade, J. G.; Schleyer, P. v. R. J Am Chem Soc 1981, 103, 5609; (d) Clark, T.; Chandrasekhar, J.; Spitznagel, G. W.; Schleyer, P. v. R. J Comput Chem 1983, 4, 294; (e) Curtiss, L. A.; McGrath, M. P.; Blaudeau, J. P.; Davis, N. E.; Binning, R. C., Jr.; Radom, L. J Chem Phys 1995, 103, 6104.

17. (a) Fukui, K. Acc Chem Res 1981, 14, 363; (b) Gonzalez, C.; Schlegel, H. B. J Phys Chem 1989, 90, 2154; (c) Gonzalez, C.; Schlegel, H. B. J Phys Chem 1990, 94, 5523.
18. Benson, S. W. Thermochemical Kinetics; Wiley-Interscience; New York, 1976.
19. Weinhold, F.; Carpenter, J. E. The Structure of Small Molecules and Ions; Plenum: New York, 1988.
20. Fujimoto, H.; Kato, S.; Yamabe, S.; Fukui, K. J Chem Phys 1974, 60, 572.
21. López, R.; Menéndez, M. I.; Suárez, D.; Sordo, T. L.; Sordo, J. A. Comput Phys Commun 1993, 76, 235.
22. Shul, R. J.; Passarella, R.; DiFazio, L. T., Jr.; Keesee, R. G.; Castleman, A. W., Jr. J Phys Chem 1988, 92, 4947.
23. The mean lives of **MA2** and **MA4** intermediates were estimated as $\tau = 1/k_{\text{diss}}$, where k_{diss} is the kinetic constant for the fragmentation of the **MA2** and **MA4** structures to $CO + H_3O$. k_{diss} was computed using the conventional transition state theory: $k_{\text{diss}} = (kT/h)\exp(-\Delta G^{\#}/RT)$, where $\Delta G^{\#}$ is the Gibbs energy barrier for the fragmentation as shown in Table I.